I.L. SEMENOV
E.O. Paton Electric Welding Institute
(11, Bozhenko Str., Kyiv 03680, Ukraine; e-mail: isemenov.paton@gmail.com)

PACS 52.27.Lw

ION DRAG FORCE ON A CHARGED MACROPARTICLE IN COLLISIONLESS PLASMA

The problem of calculating the ion drag force acting on a charged macroparticle in collisionless flowing plasma is studied by using an approach based on the direct numerical solution of the Vlasov kinetic equations for plasma components. A uniform plasma flow past a spherical macroparticle is considered. The computations are carried out for different particle sizes and different flow velocities. On the basis of the obtained results the effect of particle size on the ion drag force is analyzed. It is shown that when the particle size is much less than the Debye length in plasma, the ion drag force can be calculated with good accuracy by means of the conventional binary collision approach. A modified version of the binary collision approach is proposed to calculate the ion drag force in the case where the particle size becomes comparable to the Debye length in plasma. It is shown that there is a reasonable agreement between the results obtained using the numerical solution of the kinetic equations and that obtained by the modified binary collision approach.

K e y w o r d s: ion drag force, collisionless plasma, binary collision approach

1. Introduction

A study of the drag force exerted on a charged macroparticle by ions in flowing plasma (ion drag force) is one of the important problems in the physics of dusty plasmas. Accurate calculations of this force are necessary for understanding the basic features of dusty plasmas, such as the location and the configuration of dust structures [1–3], properties of low-frequency waves in dusty plasmas [4–6], and interaction between dust particles [7, 8]. The problem of calculating the ion drag force is rather complicated, because the value of this force is strongly affected by several factors such as collisions between plasma components, the distribution of the electric potential around a charged particle, the degree of coupling between ions and the particle, *etc.* As was shown recently [9–11], the effect of collisions between plasma components (mainly ion-neutral collisions) on the drag force is probably the most important factor in this case. However, despite the significance of this problem, a comprehensive model for the ion drag force, describing all regimes of interest, has not yet been proposed, even for collisionless plasma.

The conventional method of calculating the ion drag force in the collisionless limit is the binary collision approach [1, 12–15]. This approach is based on the study of ion scattering in the electric field of a charged particle. The scattering process is usually characterized by the scattering parameter $\beta = qe/mv^2\lambda$, where q is the particle charge, m is the ion mass, v is the average velocity of ions, and λ is the screening length of the particle charge. In the limit $\beta \ll 1$, the classical Coulomb scattering theory can be used. Such an approach was first proposed in [1] to describe the transport of dust particles in glow-discharge plasmas. The extension of this approach to the case of moderate scattering parameters ($\beta \sim 1$) was proposed in [13, 15]. In spite of the fact that this method is based on phenomenological arguments, it shows very good agreement with numerical calculations presented in [12] up to $\beta \sim 5$. In the limit $\beta \gg 1$, the classical scattering theory is not applicable, and the problem of calculating the ion drag force requires a totally different approach, which was proposed in [14].

It should be noted, however, that the binary collisional approach developed in [1, 12–15] allows one to calculate the ion drag force only when the characteristic particle size a is much less than the Debye length $r_{\rm D}$ in plasma. In this case, the electric potential around a charged particle can be taken in the well-known Yukawa form. On the other hand, it is known that when the particle size becomes comparable with the Debye length in plasma, the distribution of the electric potential around a particle deviates significantly from the Yukawa potential [16]. Generally, in order to obtain the distribution of the potential when $a \sim r_{\rm D}$, one has to solve the full nonlinear screening problem. Note that the same problem arises in calculating the floating potential of particles in plasma. In the limit $a \ll r_{\rm D}$, the floating potential can be obtained, by using the conventional orbital motion limited theory [17–19]. As was shown in [20], this approach is intrinsically inconsistent, because it does not consider peculiarities of the electric potential distribution around the particle. As a result, it cannot be used to calculate the floating potential when $a \sim r_{\rm D}$. A modified version of the orbital motion limited theory, which allows one to obtain the floating potential in this case, was proposed recently in [21]. However, as far as the author knows, the problem of calculating the ion drag force for particles with radius $a \sim r_{\rm D}$ has not yet been studied in detail so far.

In the present paper, the problem of calculating the ion drag force acting on a charged macroparticle in collisionless flowing plasmas is studied, by using an approach based on the direct numerical solution of the Vlasov equations for plasma components. This approach has been successfully used in our previous works [22, 23] to study the charging and the screening of particles in plasma without flow. In this work, a uniform flow of ions and electrons past a spherical macroparticle is studied. The numerical computations are carried out for different particle sizes and different flow velocities. On the basis of the obtained results, the influence of the particle size on the ion drag force is analyzed. It is also shown how the conventional binary collisional approach can be extended to calculate the ion drag force acting on particles with radius comparable to the Debye length in plasma.

2. Formulation of the Problem

Let us consider a spherical macroparticle of radius a inserted in a uniform plasma flow. The plasma comprises of singly charged ions (i) and electrons (e). The plasma flow far from the particle is characterized by the velocity u, temperatures $T_{\alpha 0}$ and concentrations $n_{\alpha 0}$, where $\alpha = \rm i, e$ denotes the type of plasma particle. It is assumed, that the particle is charged by plasma currents, and the particle surface is considered to be perfectly conducting. It also assumed that the flow around the particle is steady-state and axisymmetric.

The behavior of ions and electrons is described on the basis of the Vlasov equations for collisionless plasma. The problem for these equations is formulated with the use the following coordinate system. In the physical space, the cylindrical coordinates (x, r, θ), where the axis x is directed along the flow velocity, and (r, θ) are the polar coordinates in the plane perpendicular to the axis x. The center of the particle is located at the origin of the coordinate system. In the velocity space, one can use the corresponding rectangular coordinate system $(\xi_x, \xi_r, \xi_\theta)$, where ξ_x is the velocity directed along the x axis, ξ_r is the radial velocity, and ξ_θ is the azimuthal velocity. However, as was shown in [24, 25], it is more relevant to use a circular coordinate system for the radial and azimuthal velocities for the numerical solution of kinetic equations. Thus, the polar coordinates (ξ, ω) are used, where $\xi_r = \xi \cos\omega$, $\xi_\theta = \xi \sin\omega$.

Then the kinetic equations for ions and electrons are as follows:

$$\left\{L_c + L_i + \frac{q_\alpha}{m_\alpha} L_f\right\} f_\alpha = 0, \quad \alpha = \rm e, i. \tag{1}$$

Here, f_α is the velocity distribution function of the plasma particles; q_α is the particle electric charge; m_α is the particle mass; and L_c, L_i, and L_f are the convective, inertia, and force terms, respectively. These terms are

$$L_c = \xi_x \frac{\partial}{\partial x} + \xi \cos\omega \frac{\partial}{\partial r}, \quad L_i = -\frac{\xi \sin\omega}{r}\frac{\partial}{\partial \omega}, \tag{2a}$$

$$L_f = -\frac{\partial \varphi}{\partial x}\frac{\partial}{\partial \xi_x} - \frac{\partial \varphi}{\partial r}\frac{\partial}{\partial \xi_r}, \tag{2b}$$

where φ is the self-consistent electric potential, and the derivative $\partial/\partial\xi_r$ is given by

$$\frac{\partial}{\partial \xi_r} = \cos\omega \frac{\partial}{\partial \xi} - \frac{\sin\omega}{\xi}\frac{\partial}{\partial \omega}.$$

The Poisson equation for the self-consistent electric potential reads

$$\Delta\varphi = -4\pi e\,(n_{\rm i} - n_{\rm e}), \tag{3}$$

where $n_{\rm i}$ and $n_{\rm e}$ are the concentrations of ions and electrons, respectively; and the Laplacian is given by

$$\Delta = \frac{\partial^2}{\partial x^2} + \frac{1}{r}\frac{\partial}{\partial r}\left(r\frac{\partial}{\partial r}\right).$$

The basic macroscopic quantities of plasma particles such as concentrations n_α, velocities $\mathbf{u}_\alpha$, and temperatures T_α are obtained by evaluating the velocity moments of the distribution functions:

$$n_\alpha = \langle f_\alpha \rangle, \tag{4a}$$
$$n_\alpha \mathbf{u}_\alpha = \langle\, \boldsymbol{\xi}\, f_\alpha \,\rangle, \tag{4b}$$
$$3\,k\,T_\alpha n_\alpha = \langle\, m_\alpha\, \mathbf{c}_\alpha^2\, f_\alpha \,\rangle, \tag{4c}$$

where $\alpha = {\rm e}, {\rm i}$ denotes the type of the plasma particle; $\boldsymbol{\xi} = (\xi_x, \xi_r, \xi_\theta)$ is the molecular velocity; $\mathbf{c}_\alpha = \boldsymbol{\xi} - \mathbf{u}_\alpha$ is the relative velocity; and the following notation is used:

$$\langle\bullet\rangle = \int\limits_{-\infty}^{\infty}\int\limits_{0}^{\infty}\int\limits_{0}^{2\pi} \bullet\ \xi\ d\xi_x\, d\xi\, d\omega\,.$$

Note that, for the problem under consideration, the distribution functions are even in ω, i.e., $f_\alpha(\omega) = f_\alpha(-\omega)$. Thus, the tangential component of the macroscopic velocity u_α^θ equals to zero, and the velocity vector has only two nonzero components: $\mathbf{u}_\alpha = (u_\alpha^x, u_\alpha^r, 0)$.

Let us further describe the boundary conditions for Eqs. (1) and (3). As in the theory of probes, the ions and the electrons are assumed to be fully absorbed by the particle. Hence, the boundary conditions for the distribution functions on the particle surface are

$$f_\alpha = 0, \quad \alpha = {\rm e}, {\rm i}, \tag{5}$$

for $(\boldsymbol{\xi}\,\mathbf{n}) \geq 0$, where $\mathbf{n}$ is the outward unit normal to the surface. The absorption of ions and electrons by the particle leads to its charging. Since the surface of a perfectly conducting particle must be equipotential, the following boundary condition for the electric potential on the particle surface is used:

$$\varphi = \varphi_p. \tag{6}$$

Here, φ_p is the floating potential. The value of floating potential is constrained by the Gauss law:

$$4\pi q = -\int \nabla\varphi\, \mathbf{n}\, ds, \tag{7}$$

where q is the particle charge and the integral is taken over the whole particle surface.

The electric potential at large distances from the particle may be assumed to be zero, i.e., the following condition is used:

$$\varphi \to 0,\ \ (x^2 + r^2)^{1/2} \to \infty. \tag{8}$$

The boundary condition for the electric potential along the symmetry axis is

$$\partial\varphi/\partial r = 0, \tag{9}$$

at $r = 0$, $x \leq -a$, and $x \geq a$. The distribution functions of plasma components far from the particle are given by

$$M_{\alpha 0} = n_{\alpha 0} \exp\left(-\mathbf{c}_0{}^2/v_{\alpha 0}^2\right)/(\sqrt{\pi} v_{\alpha 0})^3,$$

$$(x^2 + r^2)^{1/2} \to \infty, \tag{10}$$

where $\alpha = {\rm e}, {\rm i}$ denotes the type of a plasma particle; $\mathbf{c}_0 = \boldsymbol{\xi} - \mathbf{u}_0$ is the relative velocity; $\mathbf{u}_0 = (u, 0, 0)$ is the velocity vector of the plasma flow; and $v_{\alpha 0} = \sqrt{2kT_{\alpha 0}/m_\alpha}$ are the thermal velocities in the surrounding plasma. The boundary condition for the distribution functions along the symmetry axis reads

$$f_\alpha(\xi_r) = f_\alpha(-\xi_r),\ \xi_r \geq 0, \quad \alpha = {\rm e}, {\rm i}, \tag{11}$$

at $r = 0$, $x \leq -a$, and $x \geq a$.

As was mentioned above, the distribution functions f_α are even in ω. Thus, the problem is considered only in the half-space $0 \leq \omega \leq \pi$ $(\xi_\theta \geq 0)$, by using the following symmetry boundary condition:

$$f_\alpha(\omega) = f_\alpha(-\omega), \quad \alpha = {\rm e}, {\rm i} \tag{12}$$

for $\xi \geq 0$, $-\infty < \xi_x < \infty$. In addition, one also has to define the boundary conditions at infinity in the velocity space. In this case, the following conventional assumption is used:

$$f_\alpha \to 0, \quad (\xi_x^2 + \xi^2)^{1/2} \to \infty, \quad \alpha = {\rm e}, {\rm i}. \tag{13}$$

3. Numerical Method

Further, let us briefly describe the numerical procedure used to solve Eqs. (1) and (3) with the boundary conditions (5), (6), (8)–(13). To obtain the solution of the steady-state kinetic equations (1), the author proposes to consider the time-dependent equations

$$\left\{\frac{\partial}{\partial t} + L_c + L_i + \frac{q_\mathrm{i}}{m_\mathrm{i}} L_f\right\} f_\mathrm{i} = J_\mathrm{i}, \tag{14a}$$

$$\left\{\frac{\partial}{\partial t_\mathrm{e}} + L_c + L_i + \frac{q_\mathrm{e}}{m_\mathrm{e}} L_f\right\} f_\mathrm{e} = J_\mathrm{e},, \tag{14b}$$

where $t_\mathrm{e} = t\, v_{\mathrm{i}0}/v_{\mathrm{e}0}$, and $v_{\mathrm{i}0}$, $v_{\mathrm{e}0}$ are the thermal velocities of ions and electrons in the surrounding plasma. The initial conditions for Eqs. (14) are given by the Maxwell functions (10), and the boundary conditions are given by Eqs. (5), (10), (11), (12), and (13). The distribution of the electric potential at each moment of time is calculated using the Poisson equation (3) with the boundary conditions (6), (8), and (9). In order to obtain the particle charge, Eqs. (14) are supplemented with the charging equation

$$dq/dt = -\int \mathbf{j}\,\mathbf{n} ds, \tag{15}$$

where $\mathbf{j} = e(n_\mathrm{i}\mathbf{u}_\mathrm{i} - n_\mathrm{e}\mathbf{u}_\mathrm{e})$ is the current density, and the integral is taken over the whole particle surface.

In the steady state, Eqs. (14) are reduced to the stationary equations (1). Thus, in order to obtain the solution of the flow problem under consideration, Eqs. (14) are solved in time until a steady-state solution is reached. Note that Eqs. (14) differ from the conventional system of time-dependent Vlasov equations for plasma particles. One can see that the time derivative term in the equation for electrons (14b) is multiplied by the scaling factor $v_{\mathrm{e}0}/v_{\mathrm{i}0}$. It is required to overcome the difficulty caused by a great difference between the time scales for ions and electrons. Equations (14) do not describe a real physical process, but it can be viewed just as a tool for finding the stationary solution of the problem, which is believed to be unique. It is worth noting that the same technique for finding a steady-state solution of the kinetic equations was successfully used in our previous works [22, 23] devoted to the study of the charging and screening processes.

In the physical space, Eqs. (1) and (3) are solved in a finite domain

$$\Omega_p = \left\{a \le (x^2 + r^2)^{1/2} \le A_R,\ r \ge 0\right\}. \tag{16}$$

In the velocity space, the kinetic equations for ions and electrons are solved in finite domains Ω_v^i and Ω_v^e, respectively, where

$$\Omega_v^\alpha = \left\{\begin{matrix} -A^\alpha_{\xi_x} \le \xi_x \le A^\alpha_{\xi_x}, \\ 0 \le \xi \le A^\alpha_\xi, \\ 0 \le \omega \le \pi \end{matrix}\right\},\ \alpha = \mathrm{e}, \mathrm{i}. \tag{17}$$

The sizes A_R, $A^\alpha_{\xi_x}$, and A^α_ξ are chosen sufficiently large to capture the boundary conditions (8), (10) and (13). The basic equations are discretized using a nonstructured nonuniform triangular mesh in the physical space and uniform finite-volume meshes in the velocity space. The nonuniform triangular mesh is created using the approach proposed in [26].

The numerical procedure for solving Eqs. (14) is based on the method of operator splitting. Below, this method is described on the example of the kinetic equation for ions (14a). This equation is solved by means of the following two-stage splitting scheme. At the first stage, the action of the operator L_c at each discrete velocity node $(\xi_x^{(l)}, \xi^{(l)}, \omega^{(l)})$ is considered, where l denotes the number of the node. The corresponding equation is

$$\left\{\frac{\partial}{\partial t} + L_c^{(l)}\right\} f_\mathrm{i}^{(l)} = 0, \tag{18}$$

where $f_\mathrm{i}^{(l)}$ is the distribution function at the velocity node, and the operator $L_c^{(l)}$ is given by

$$L_c^{(l)} = \xi_x^{(l)} \frac{\partial}{\partial x} + \xi^{(l)} \cos(\omega^{(l)}) \frac{\partial}{\partial r}. \tag{19}$$

Equation (18) with the boundary conditions (5), (10), and (11), which are imposed at the respective boundaries of the computational domain Ω_p, is solved numerically by the explicit MUSCL-type finite volume scheme for nonstructured meshes proposed in [27] (the maximum limited gradient scheme).

At the second stage, the action of the inertia and force terms at each discrete node $(x^{(j)}, r^{(j)})$ in the physical space is considered. Here, j denotes the number of the triangle, and $(x^{(j)}, r^{(j)})$ is the node of a finite volume mesh located at the center of the triangle. The corresponding equation reads

$$\left\{\frac{\partial}{\partial t} + L_i^{(j)} + L_f^{(j)}\right\} f_\mathrm{i}^{(j)} = 0, \tag{20}$$

where $f_{\rm i}^{(j)}$ is the distribution function at the discrete node, and the operators $L_i^{(j)}$ and $L_f^{(j)}$ are given by

$$L_i^{(j)} = -\frac{\xi \sin\omega}{r^{(j)}} \frac{\partial}{\partial \omega}, \tag{21a}$$

$$L_f^{(j)} = -\Big(\frac{\partial \varphi}{\partial x}\Big)^{(j)} \frac{\partial}{\partial \xi_x} - \Big(\frac{\partial \varphi}{\partial r}\Big)^{(j)} \frac{\partial}{\partial \xi_r}. \tag{21b}$$

The derivatives of the potential at the center of a triangle are calculated from the solution of the Poisson equation (3). Equation (20) with the boundary conditions (12), (13) is solved numerically, by using the explicit MUSCL-type finite volume scheme with a superbee slope limiter [28].

The Poisson equation (3) with boundary conditions (8) and (9) and the floating potential constraint (6), (7) is solved by the finite element method with quadratic Lagrangian elements [29]. The particle charge is obtained, by using Eq. (15), which is solved by the explicit Euler method. The kinetic equation for electrons (14b) is solved, by using the same method, as was described above for the ions. In order to hasten the computational process, the parallel version of the proposed numerical method has been developed, by using a shared-memory parallelization technique. The method is parallelized as follows. During the first stage of the splitting scheme [see Eq. (18)], the computing threads operate on different domains in the velocity space. During the second step [see Eqs (20)], the threads operate on different sets of triangles in the physical space. The proposed algorithm was found to be very effective, because it involves the parallelization both in the velocity and physical spaces. The algorithm was implemented, by using the OpenMP library.

4. Results and Discussions

In this section, the results of computations performed by means of the proposed numerical method are summarized and discussed. It should be noted that the problem under consideration was solved in the dimensionless form, i.e., there is no need to specify the values of background plasma parameters such as $n_{\alpha 0}$, $T_{\alpha 0}$ and u. For simplicity, the case of isothermal plasma flow was considered, i.e., it was assumed that $T_{\rm e0} = T_{\rm i0}$. The flow velocity was varied below $v_{\rm i0}$. The particle radius was chosen to be $a = 0.2 r_{\rm D}$, $a = 0.5 r_{\rm D}$, and $a = r_{\rm D}$, where $r_{\rm D}$ is the Debye length in plasma:

$$r_{\rm D}^{-2} = 4\pi e^2 \left(n_{\rm e0}/kT_{\rm e0} + n_{\rm i0}/kT_{\rm i0}\right). \tag{22}$$

In all calculations, the dimension of the computational domain in the physical space A_R was varied around $20 r_{\rm D}$. The number of triangles was varied from 1500 to 2000, and the average number of nodes on the particle surface was 20. The sizes of the computational domains in the velocity space A_ξ^α and $A_{\xi_x}^\alpha$ were varied from $4 v_{\alpha 0}$ to $6 v_{\alpha 0}$, $\alpha = {\rm e}, {\rm i}$. The step sizes of the finite-volume mesh in the velocity space were $\Delta\xi = \Delta\xi_x = 0.25\, v_{\alpha 0}$, and the number of nodes on the interval $0 \le \omega \le \pi$ was 20. The number of computing threads was chosen to be 32 or 64. The total computational time required to obtain the steady-state solution of the flow problem under consideration was varied from 2 to 4 h.

The main focus of this work is on the drag force exerted on a particle by ions. Note that the electron drag force can be usually neglected owing to the great difference between the ion and electron masses. According to the conventional terminology, the ion drag force $\mathbf{F}_d$ is given by the sum of two components,

$$\mathbf{F}_d = \mathbf{F}_m + \mathbf{F}_e, \tag{23}$$

where $\mathbf{F}_m$ is the force arising due to the mechanical interaction between ions and the particle surface, and $\mathbf{F}_e$ is the force arising from the interaction of the particle charge with the flow-induced plasma anisotropy. The first component is

$$\mathbf{F}_m = -\int \mathcal{P}_{\rm i}\, \mathbf{n}\, ds, \tag{24}$$

where $P_{\rm i}$ is the stress tensor for ions given by

$$\mathcal{P}_{\rm i} = m_{\rm i} \left\langle \boldsymbol{\xi} \otimes \boldsymbol{\xi}\, f_{\rm i} \right\rangle r. \tag{25}$$

The second component reads

$$\mathbf{F}_e = \int \mathcal{M}\, \mathbf{n}\, ds, \tag{26}$$

where $\mathcal{M}$ is the Maxwell stress tensor

$$\mathcal{M} = \frac{1}{4\pi} \left\{ \mathbf{E} \otimes \mathbf{E} - \frac{1}{2} \mathbf{E}^2 \right\}, \tag{27}$$

and $\mathbf{E} = -\nabla\varphi$ is the vector of the electric field. Since the flow around the particle is axisymmetric,

ISSN 2071-0194. Ukr. J. Phys. 2013. Vol. 58, No. 3

the ion drag force is directed along the axis of symmetry. Hence, one can consider only the x component of this force and denote, for brevity, $F_d \equiv (\mathbf{F}_d)_x$, $F_e \equiv (\mathbf{F}_e)_x$, $F_m \equiv (\mathbf{F}_m)_x$.

In order to clarify the nature of the electric component F_e, the distributions of the normalized charge density along the axis of symmetry are shown in Fig. 1 for $u = 0.5v_{\mathrm{i0}}$ and different particle sizes. The normalized charge density is given by $\Delta\rho/\rho_{\mathrm{i0}}$, where $\Delta\rho = e\,(n_{\mathrm{i0}} - n_{\mathrm{e}})$ and $\rho_{\mathrm{i0}} = en_{\mathrm{i0}}$. In Fig. 1 one can observe anisotropy in the distribution of the charge density around the particle. It can be seen that the charge density in the wake region behind the particle ($x > a$) is higher than the charge density in front of the particle ($x < -a$). Taking into account that the particle charge is usually negative due to the much higher mobility of electrons than that of ions in the plasma, one can conclude that there exists a non-zero force F_e acting on a particle from the anisotropic electric field. It is clear from Fig. 1 that this force is usually positive, i.e., it is directed along the plasma flow. One can also see that the anisotropy in the distribution of the charge density becomes less pronounced as the particle size increases. Hence, the force F_e should decrease, as the ratio a/r_{D} increases. It is also worth noting that, in typical laboratory dusty plasmas, the electric force F_e is usually much higher than the mechanical force F_m.

Further, let us discuss the dependence of the ion drag force on the particle size. As was mentioned in the introduction, the ion drag force can be calculated in the case where $a \ll r_{\mathrm{D}}$ by means of the binary collision approach [1, 12–15]. According to this approach, the ion drag force F_{bc} is given by the sum of two components,

$$F_{bc} = F_{bc}^{c} + F_{bc}^{o}, \tag{28}$$

where F_{bc}^{c} is the collection part associated with the momentum transfer from the ions that collide with the particle, and F_{bc}^{o} is the orbital part, which is due to the momentum transfer from the ions that are scattered in the electric field of the particle. The collection component F_{bc}^{c} is calculated by the conventional orbital motion limited theory:

$$F_{bc}^{c} = \sqrt{\pi}a^2 p_{\mathrm{i0}}\hat{u}^{-2}\Big\{\hat{u}\left(1 + 2\hat{u}^2 + 2\hat{\varphi}_p\right)e^{-\hat{u}^2} +$$

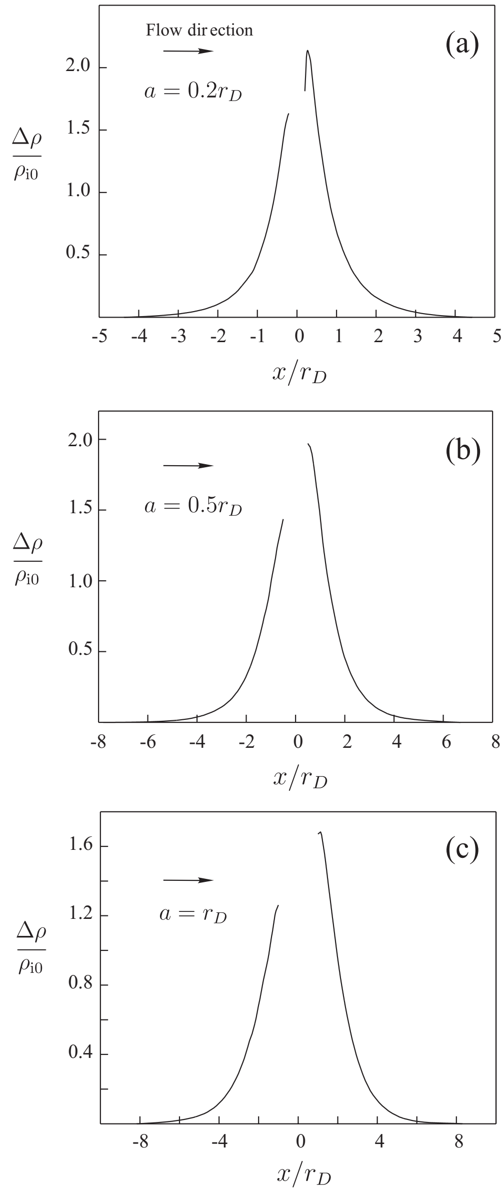

Fig. 1. Distributions of the normalized charge density along the axis of symmetry for $u = 0.5v_{\mathrm{i0}}$ and different particle sizes: $a = 0.2r_{\mathrm{D}}$ (*a*), $0.5r_{\mathrm{D}}$ (*b*), r_{D} (*c*). The arrow shows the flow direction. The normalized charge is given by $\Delta\rho/\rho_{\mathrm{i0}}$, where $\Delta\rho = e(n_{\mathrm{i}} - n_{\mathrm{e}})$ and $\rho_{\mathrm{i0}} = n_{\mathrm{i0}}e$. Note that, far from the particle, the quasineutrality condition holds $n_{\mathrm{i0}} = n_{\mathrm{e0}}$

$$+\left[4\hat{u}^4 + 4\hat{u}^2 - 1 - 2\left(1 - 2\hat{u}^2\right)\hat{\varphi}_p\right]\frac{\sqrt{\pi}}{2}\mathrm{erf}(\hat{u})\Big\}, \tag{29}$$

where $\hat{\varphi}_p = |\varphi_p|/kT_{\mathrm{i0}}$ is the normalized particle potential, and $\hat{u} = u/v_{\mathrm{i0}}$ is the normalized flow veloc-

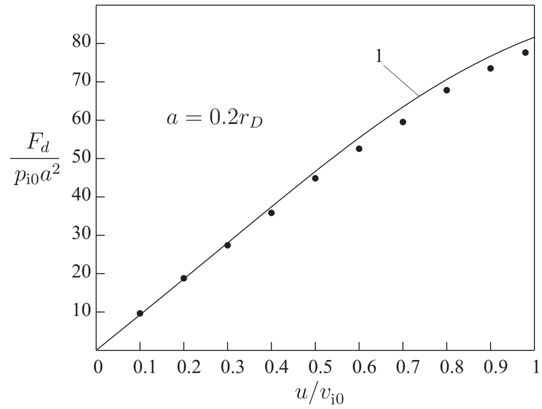

Fig. 2. Velocity dependence of the ion drag force for $a = 0.2r_{\rm D}$. Symbols • show the present results. Solid line (1) shows the results obtained by the conventional binary collision approach [see Eqs. (28), (29), and (30)]

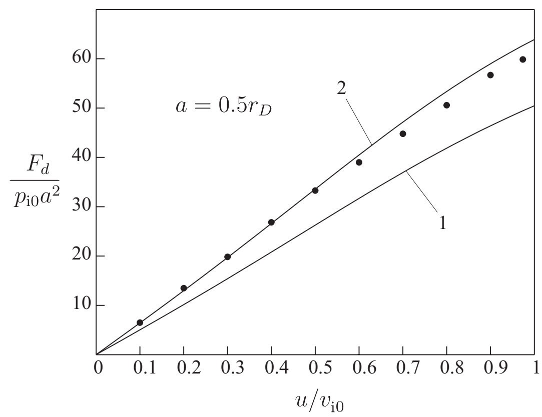

Fig. 3. Velocity dependence of the ion drag force for $a = 0.5r_{\rm D}$. Symbols • show the present results. Solid line (1) shows the results obtained by the conventional binary collision approach [see Eqs. (28), (29), and (30)]. Solid line (2) shows the results obtained by the modified binary collision approach [see Eqs. (33), (29), and (34)]

ity. The orbital component is calculated, by using the modified Coulomb scattering theory:

$$F^o_{bc} = 8\pi\, n_{i0}\, \frac{q_i^2\, {\varphi_p}^2}{m_i v_{i0}^2}\, a^2 G\,(u/v_{i0}) \ln\Lambda, \tag{30}$$

where

$$G(x) \equiv \left[\sqrt{\pi}\,{\rm erf}(x)/2 - \, x\, e^{-x^2}\right]/(\sqrt{\pi}x^2)$$

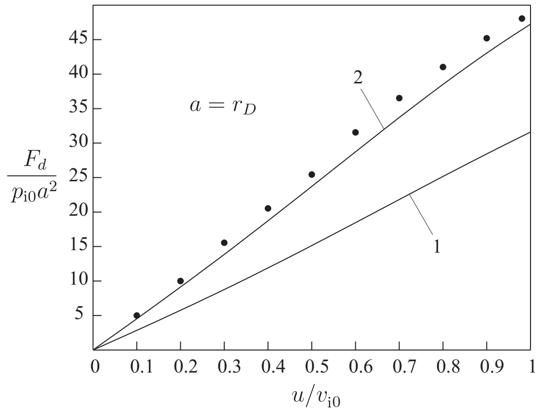

Fig. 4. Velocity dependence of the ion drag force for $a = r_{\rm D}$. Symbols • show the present results. Solid line (1) shows the results obtained by the conventional binary collision approach [see Eqs. (28), (29) and (30)]. Solid line (2) shows the results obtained by the modified binary collision approach [see Eqs. (33), (29), and (34)]

is the Chandrasekhar function; and $\ln\Lambda$ is the modified Coulomb logarithm given by the relation

$$\ln\,\Lambda = \ln\left[\frac{b_s + \lambda_s}{b_s + a}\right], \tag{31}$$

where

$$b_s = a\, e\, |\varphi_p|/\left(2T_{i0} + m_i u^2\right),$$

$$\lambda_s^2 = r^2_{\rm D_e}/\left[1 + T_{e0}/\left(T_{i0} + m_i u^2\right)\right],$$

$$r^{-2}_{\rm D_e} = 4\pi e^2 n_{e0}/kT_{e0}. \tag{32}$$

In Fig. 2, the dependence of the normalized ion drag force on the normalized flow velocity u/v_{i0} is shown for $a = 0.2r_{\rm D}$. The normalized ion drag force is defined as $F_d/p_{i0}a^2$, where $p_{i0} = n_{i0}kT_{i0}$. The filled symbols on this figure (•) indicate the present results obtained by the numerical solution of the kinetic equations. The solid line (1) shows the results obtained using the conventional binary collisional approach, i.e., by Eqs. (28), (29), and (30). Since the ratio $a/r_{\rm D}$ is sufficiently small in this case, the binary collisional theory is expected to give accurate results. In fact, one can see from Fig. 2 that there is the good agreement between the kinetic results and those obtained by the binary collision approach. However, the situation changes as the particle size increases.

In Figs. 3–4, the dependence of the normalized ion drag force on the normalized flow velocity is shown for $a = 0.5r_{\rm D}$ and $a = r_{\rm D}$, respectively. Once again, the filled symbols (•) indicate the present results obtained by the numerical solution of the kinetic equations, and the solid line (1) shows the results obtained by the binary collisional approach, i.e., by Eqs. (28), (29), and (30). One can see from these figures that the conventional binary collision theory becomes inapplicable, as the ratio a/r_{D} increases. In author's opinion, it can be explained by the following two facts. First, the binary collision approach does not consider the effect of a particle size on the distribution of the electric potential around a particle. As was mentioned before, this approach is based on the assumption that the distribution of the potential has the well-known Yukawa form. It is known, however, that the potential of particles with radius $a \sim r_{\mathrm{D}}$ decays more slowly than the Yukawa potential. Second, the binary collision theory does not consider the effect of the particle size on the screening length λ_s [see Eq. (32)]. However, as it was shown in [30], the screening length becomes greater than that obtained from the solution of the linearized problem, as the ratio a/r_{D} increases.

In order to extend the binary collision approach to the case of particles with radius comparable to the Debye length in plasma, the author proposes a modified version of this method, which takes the disadvantages mentioned above into account. The modified expression for the ion drag force reads

$$F_{bc} = F_{bc}^{c} + \tilde{F}_{bc}^{o}, \tag{33}$$

where the collection part F_{bc}^{c} is given by Eq. (29), and the orbital part is given by

$$\tilde{F}_{bc}^{o} = 8\pi\, n_{\mathrm{i}0}\, \frac{q_{\mathrm{i}}^{2}\, \tilde{\varphi}_p^{\,2}}{m_{\mathrm{i}} v_{\mathrm{i}0}^{2}}\, a^{2} G\left(u/v_{\mathrm{i}0}\right) \ln \Lambda, \tag{34}$$

where $\tilde{\varphi}_p$ is the modified surface potential. The Coulomb logarithm is given by

$$\ln \Lambda = \ln \left[\frac{b_s + \tilde{\lambda}_s}{b_s + a}\right], \tag{35}$$

where

$$\tilde{\lambda}_s^{2} = a^{2} + r_{\mathrm{D_e}}^{2} / \left[1 + T_{\mathrm{e}0} / \left(T_{\mathrm{i}0} + m_{\mathrm{i}} u^{2}\right)\right]. \tag{36}$$

The modified surface potential is chosen in such a way that the product $\tilde{\varphi}_p a$ is equal to the actual particle charge q. Note that the linear relation $q = a\varphi_p$, which is valid in the limit $a/r_{\mathrm{D}} \to 0$, does not hold for sufficiently large particles ($a \sim r_{\mathrm{D}}$). As the ratio a/r_{D} increases, the particle charge becomes higher than $a\varphi_p$. This effect can be taken into account with the use of a modified value of surface potential ($\tilde{\varphi}_p = q/a$) in Eq. (34). Moreover, the use of the adjusted surface potential allows one to account for the fact that the particle potential decays more slowly than the Yukawa potential. The value of the actual particle charge can be obtained, for example, by means of the nonlinear collisionless model proposed in [16]. In addition, the author proposes to use the modified screening length given by Eq. (36), which allows one to account for the effect of the particle size on the screening length of the particle charge in the plasma.

The solid line (2) in Figs. 2 and 3 shows the results obtained by the modified binary collision approach described above. One can observe that there is a reasonable agreement between the results obtained with the use of the numerical solution of the kinetic equations and those obtained by Eqs. (33)–(36). Thus, one can conclude that the modified binary collision approach proposed in this paper is more accurate than the conventional binary collision approach and allows one to calculate the ion drag force in the case where the particle size is comparable to the Debye length in plasma. It should be noted that the author do not expect this approach to work in the limit $a/r_{\mathrm{D}} \to \infty$. In this case, however, the electric part of the ion drag force becomes negligibly small, and the value of ion drag force is completely determined by its mechanical part.

5. Conclusion

The present work is devoted to the problem of calculating the drag force exerted on a charged macroparticle by ions in flowing plasma (ion drag force). The problem is studied by using an approach based on the direct numerical solution of the Vlasov kinetic equations for plasma components. The author considers a uniform flow of plasma consisting of ions and electrons past a spherical macroparticle, which is charged by plasma currents. The computations were performed for different particle sizes and different flow velocities. Using the obtained results, the influence of the particle size on the ion drag force is analyzed. It is shown that, for sufficiently small particles, i.e., when $a \ll r_{\mathrm{D}}$, the ion drag force can be calculated with good accuracy by the conventional binary collision approach. As the ratio a/r_D increases, the results obtained with the use of this method deviates noticeably from that obtained by means of the numerical solution of the kinetic equations. It is explained by the fact that the conventional binary collisional approach does not consider the effect of the particle size on the distribution of the electric potential around the particle and the screening length of the particle charge in plasma. In order to account for the effect of the particle size, a modified version of the binary collision approach is proposed. It is shown that there is a reasonable agreement between the results obtained by the solution of the kinetic equations and those obtained by the modified binary collision approach in the case where the particle size becomes comparable to the Debye length in plasma.

The work was supported by the joint grant of the National Academy of Sciences of Ukraine and the Russian Fund of Fundamental Researches.

1. M.S. Barnes, J.H. Keller, J.C. Forster, J.A. O'Neill, and D.K. Coultas, Phys. Rev. Lett. **68**, 313 (1992).
2. G.E. Morfill, H.M. Thomas, U. Konopka, H. Rothermel, M. Zuzic, A. Ivlev, and J. Goree, Phys. Rev. Lett. **83**, 1598 (1999).
3. S.V. Vladimirov and N.F. Cramer, Phys. Rev. E **62**, 2754 (2000).
4. N. D'Angelo, Phys. Plasmas **5**, 3155 (1998).
5. A.V. Ivlev, D. Samsonov, J. Goree, G. Morfill, and V.E. Fortov, Phys. Plasmas **6**, 741 (1999).
6. S.A. Khrapak and V.V. Yaroshenko, Phys. Plasmas **10**, 4616 (2003).
7. V.N. Tsytovich, Phys. Usp. **40**, 53 (1997).
8. S.A. Khrapak, A. Ivlev, and G. Morfill, Phys. Rev. E **64**, 046403 (2001).
9. S.A. Khrapak, S.K. Zhdanov, A.V. Ivlev, and G.E. Morfill, J. Appl. Phys. **101**, 033307 (2007).
10. L. Patacchini and I.H. Hutchinson, Phys. Rev. Lett. **101**, 025001 (2008).
11. A.V. Filippov, A.G. Zagorodny, A.I. Momot, A.F. Pal', and A.N. Starostin, JETP 108, **497** (2009).
12. M.D. Kilgore, J.E. Daugherty, R.K. Porteous, and D.B. Graves, J. Appl. Phys. **73**, 7195 (1993).
13. S.A. Khrapak, A.V. Ivlev, G.E. Morfill, and H.M. Thomas, Phys. Rev. E **66**, 046414 (2002).
14. S.A. Khrapak, A.V. Ivlev, G.E. Morfill, and S.K. Zhdanov, Phys. Rev. Lett. **90**, 225002 (2003).
15. S.A. Khrapak, A.V. Ivlev, S.K. Zhdanov, and G.E. Morfill, Phys. Plasmas **12**, 042308 (2005).
16. T. Bystrenko and A. Zagorodny, Phys. Lett. A **299**, 383 (2002).
17. H.M. Mott-Smith and I. Langmuir, Phys. Rev. **28**, 727, (1926).
18. U. de Angelis, Physica Scripta **45**, 465 (1992).
19. J.E. Allen, Physica Scripta **45**, 497 (1992).
20. J.E. Allen, B.M. Annaratone, and U. de Angelis, J. Plasma Physics **63**, 299 (2000).
21. C.T.N. Willis, M. Coppins, M. Bacharis, and J.E. Allen, Phys. Rev E **85**, 036403 (2012).
22. I.L. Semenov, A.G. Zagorodny, and I.V. Krivtsun, Phys. Plasmas **18**, 103707 (2011).
23. I.L. Semenov, A.G. Zagorodny, and I.V. Krivtsun, Phys. Plasmas **19**, 043703 (2012).
24. H. Sugimoto and Y. Sone, Phys. Fluids A **4**, 419 (1992).
25. L. Mieussens, J. Comput. Phys. **162**, 429 (2000).
26. P. Persson and G. Strang, SIAM Review **46**, 329 (2004).
27. P. Batten, C. Lambert, and D.M. Causon, Int. J. Num. Methods Eng. **39**, 1821 (1996).
28. E.F. Toro, *Riemann Solvers and Numerical Methods for Fluid Dynamics: A Practical Introduction* (Springer, Berlin, 2009).
29. O.C. Zienkiewicz and R. L. Taylor, *The Finite Element Method: The Basis* (Butterworth-Heinemann, Oxford, 2000).
30. J.E. Daugherty, R.K. Porteous, M.D. Kilgore, and D.B. Graves, J. Appl. Phys. **72**, 3934 (1992).

Received 10.12.12

І.Л. Семенов

ІОННА СИЛА ОПОРУ, ЩО ДІЄ НА ЗАРЯДЖЕНУ МАКРОЧАСТИНКУ В БЕЗЗІТКНЮВАЛЬНІЙ ПЛАЗМІ

Р е з ю м е

Проблема обчислення іонної сили опору, що діє на заряджену макрочастинку в потоці беззіткнювальної плазми, досліджується на основі прямого чисельного розв'язку системи кінетичних рівнянь Власова для компонент плазми. Розглянуто процес обтікання сферичної мікрочастинки рівномірним потоком плазми. Розрахунки проводяться для різних розмірів частинок та різних значень швидкості потоку плазми. На основі отриманих результатів, досліджується вплив розміру частинки на величину іонної сили опору. Показано, що коли розмір частинки набагато менший за довжину Дебая в плазмі, іонну силу опору можна обчислити з гарною точністю за допомогою відомої теорії парних зіткнень. Для обчислення іонної сили опору у випадку, коли розмір частинки стає порівняним із довжиною Дебая в плазмі, запропоновано модифіковану теорію парних зіткнень. Показано, що результати, отримані шляхом чисельного розв'язку кінетичних рівнянь, добре узгоджуються із результатами, які отримані за допомогою модифікованої теорії парних зіткнень.